Title: Jaw kinematics and mandibular morphology in humans

Myra F. Laird [a, *], Callum F. Ross [a], Paul O'Higgins [b]

[a] *Department of Organismal Biology and Anatomy, University of Chicago, Chicago, IL USA*

[b] *Centre for Anatomical & Human Sciences, Department of Archaeology and Hull York Medical School, University of York, York, UK*

*Corresponding author.

E-mail address: myra.laird@usc.edu (M.F. Laird).

Keywords: Jaw kinematics, Mandible, Geometric morphometrics

Acknowledgments

We thank Mike Plavcan, the associate editor, and two reviewers for improving the overall quality of this work. Thanks to Herman Pontzer for the use of the Hunter College Human Evolution and Energetics Laboratory. Finally, thank you to all chewing trial volunteers.

Abstract

Understanding the influence of feeding behavior on mandibular morphology is necessary for interpreting dietary change in fossil hominins. However, mandibular morphology is also likely to have an effect on feeding behavior, including jaw kinematics. Here we examine the relationships between mandibular morphology and jaw kinematics in humans using landmark-based morphometrics to quantify jaw movement. Three-dimensional movements of reflective markers coupled to the mandible and cranium were used to capture jaw movements while subjects chewed cubes of raw and cooked sweet potato. Geometric morphometric methods were adapted to quantify and analyze gape cycle motion paths. Gape cycles varied significantly across chewing sequences and between raw and cooked sweet potato. Variation in gape cycle size and shape is related to the width (intergonial distance) and length of the mandible. These results underline the fact that jaw kinematic variation within and between taxa is related to and may be influenced by mandibular morphology. Future studies examining kinematic variation should assess the influence of morphological differences on movement.

1. Introduction

Although diet and mandibular morphology have been widely studied in primates, the relationships between them remain obscure (Hylander, 1979, 1985, 1988; Bouvier and Hylander, 1981; Smith, 1983; Bouvier, 1986a,b; Daegling, 1992; Cole, 1992; Ravosa, 1996, 2000; Taylor, 2002, 2006; Vinyard et al., 2003). One possible reason may be that diet only influences mandibular morphology indirectly through variation in gross aspects of feeding behavior (Ross et al., 2012). In turn, feeding behavior is variably impacted by several aspects of diet, including food geometric and material properties, as well as by an animal's phylogenetic, ecological and sociological context (e.g., Hylander 2013). However, there is also evidence that, in humans at least, the direction of causality may in some cases be the reverse of what is traditionally assumed: i.e., mandibular morphology may affect various aspects of feeding behavior, including EMG activity and jaw kinematics (Ahlgren, 1966; Møller 1966, Ingervall and Thilander, 1974; Ingervall and Helkimo, 1978; Kiliaridis et al., 1985). This paper presents a detailed analysis of relationships between mandibular morphology and jaw kinematics in humans using a novel application of geometric morphometric techniques to kinematics.

A chewing sequence is the sequence of gape cycles from ingestion to swallow and can be divided into sequentially numbered cyclic jaw movements or gape cycles (Fig. 1). The kinematics of the gape cycle are typically measured by tracking vertical and lateral displacement of the jaw over time (e.g. Reed and Ross, 2010; Iriarte-Diaz et al., 2011; Laird, 2017). Vertical displacement of the jaw during gape cycles is thought to vary as chewing progresses within a sequence reflecting the breakdown of food particles, bolus formation, changes in external bolus properties, and changes in food material properties (Foster et al., 2006; Woda et al., 2006;

Vinyard et al., 2008). In this context, decreases in vertical displacements and variation in muscle activity amplitudes through the chewing sequence reflect the decrease in food fragment sizes and variation in bolus properties as the sequence progresses (Pruim et al., 1978; Manns et al., 1979; Hylander and Johnson, 1985; Spencer, 1998; Olmsted et al., 2005; Vinyard et al., 2008; Reed and Ross, 2010; Laird, 2017). In humans, foods with higher toughness are often associated with greater vertical and lateral jaw displacements during the gape cycle (Anderson et al., 2002; Foster et al., 2006; Wintergerst et al., 2008; Laird, 2017; but see Takada et al., 1994; Peyron et al., 1997; Reed and Ross, 2010).

What has seldom been addressed is the possibility that jaw kinematics are also impacted by the overall shape of the mandible. This is of interest because variation in a suite of features of human mandibular morphology, particularly differences in symphyseal height, overall anteroposterior length, mediolateral breadth, and the gonial angle, has been associated with geographic, climatic, dietary, and feeding performance factors (Kaifu, 1997; Nicholson and Harvati, 2006; von Cramon-Taubadel, 2011; Katz et al., 2017). When modeled as a constrained lever, variation in the length of mandible will move the dental functional area relative to the muscle resultant and change the location of maximum bite force production (Greaves, 1978; Spencer and Demes, 1993). Large vertical bite forces are associated with a short and broad mandibular ramus, a low coronoid process/shallow mandibular notch, and large bicondylar breadth (Herring and Herring, 1974). Humans with longer faces, narrower mandibles, and larger gonial angles have reduced masseter muscle thickness (Throckmorton et al., 1980, Kiliaridis and Kälebo, 1991; Van Spronsen et al., 1992). These features are thought to influence the mechanical advantage of the primary jaw adductors -- the masseter and temporalis muscles.

63 However, there is a well-documented trade-off between mechanical advantage and gape
64 such that larger gapes require greater muscle stretch and/or posteriorly positioned jaw elevator
65 muscles, negatively impacting jaw mechanical advantage (Herring and Herring, 1974; Lindauer
66 et al., 1993; Van Eijden and Turkawski, 2001; Hylander, 2013; Iriarte-Diaz et al., 2017). This
67 indicates that vertical movements of the jaw that stretch the muscles beyond their optimum
68 length result in decreased mechanical advantage and lower bite forces. Beyond this, the
69 ontogeny of the mandible is well known to be strongly influenced by its loading history (Moss
70 and Salentijn, 1969; Pearson and Lieberman, 2004), hence an association between function and
71 mandibular size and shape is to be expected.
72 We tested a series of hypotheses to investigate how gape cycle size and shape vary with cycle
73 number across a chewing sequence, food type, and measures of mandibular morphology. First,
74 gape cycles were hypothesized to change across the chewing sequence (H1), such that gape
75 cycles are larger at the beginning of the chewing sequence before the food has been broken
76 down. Gape cycles were also expected to differ between food types (in this case raw and cooked
77 sweet potato) within each subject, reflecting differences in food particle breakdown, toughness,
78 and elastic modulus. We hypothesized that raw sweet potato gape cycles will be larger than
79 cooked sweet potato gape cycles, reflecting food material property-related differences in rates of
80 particle breakdown and swallow-safe bolus formation (H2). Next, we compared jaw kinematics
81 across individuals, assessing the extent to which gape cycle variation with food type and cycle
82 number is consistent across individuals (H3). Finally, we hypothesized that differences in gape
83 cycles among individuals covary with measures of mandibular size and shape (H4). Specifically,
84 we hypothesize that smaller gape cycles are associated with greater mandibular mechanical
85 advantage and tradeoffs between gape and bite-force tradeoffs. Smaller gape cycles would allow

subjects to maximize their mechanical advantage and minimize muscular stretch. As there are likely three-dimensional complexities of jaw movement that can only be quantified and analyzed using multivariate techniques, we addressed these hypotheses using a novel application of geometric morphometric techniques to gape cycles. This allows us to quantify and compare the three-dimensional size and shape of these motions to better understand how cycle size and shape vary with cycle number, food, and morphology.

2. Materials and Methods

Chewing sequences were recorded from twelve adult human subjects (seven women and five men) between the ages of 21 and 29. Subjects were free from chronic masticatory problems, had not had dental work within the last six months, and were not missing any teeth (except for M_3's). Each subject completed chewing trials on 15 mm^3 cubes of cooked and raw sweet potato. To standardize the start of the chewing sequence, subjects completed two chewing trials in which they were asked to start chewing with the cube on their right lower first molar. Subjects were asked to chew at their normal rate only on the right side until all particles were swallowed. Side-imposed chewing reflects normal unilateral loading during mastication and allowed us to capture variation in jaw movements without differences in loading side or food movement within the mouth. The chewing trials took place at the Human Evolution and Energetics Lab at Hunter College. All subjects were volunteers and gave informed consent before participating in the study. The New York University Committee on Activities Involving Human Subjects (project number 11-8561), and the Hunter College Human Research Protection Program (project number 11-08-165-4471) granted approval for the study.

The cooked sweet potato was prepared by boiling the cubes for five minutes at 100° C. Raw and cooked sweet potato appear to differ in food toughness (the work needed to propagate a

109 crack through an object: Cooked: 57.15 ± 18.8; Raw: 841.0 ± 75.63), and elastic modulus (the
110 ratio of stress to strain within the elastic region of the food: Cooked: 0.03 ± 0.02; Raw:
111 3.65 ± 0.99)

112 *2.1 Distinguishing gape cycles*

113 A Vicon motion capture system (www.vicon.com) recording at 200 Hz was used to
114 capture the three-dimensional coordinates of a series of six reflective markers adhered to each
115 subject's face using double-sided tape directly above the following osteological landmarks:
116 pogonion, nasion, right and left condylion laterale, and right and left gonion (Fig. 2; Table 1).
117 Reflectors were placed on three subjects on two separate occasions to test intra-observer error in
118 marker placement. There were no significant differences in the pairwise distances between the
119 markers (using a Student T-Test, $p = 0.72$). Unless noted, all data formatting and analyses were
120 run in R (R Core Team, 2017).

121 Gape cycles within a chewing sequence were identified using the change in distance
122 between the three-dimensional coordinates at nasion and pogonion, which changes over time
123 with jaw opening and closing. Gape cycles were specifically defined as the sequential departure
124 from- and return to the point of minimum gape (Hiiemae, 1978; Bramble and Wake, 1985).
125 Local minima were found using the R package 'quantmod,' and the time points of these minima
126 were used to distinguish individual gape cycles throughout the chewing sequence. Jaw
127 movements with longer durations or atypical movement patterns were attributed to swallows or
128 food positioning within the mouth and were excluded. Gape cycles throughout the chewing
129 sequence were sequentially numbered (cycle number). All analyses were restricted to the first 20
130 gape cycles in the chewing sequence in order to capture the greatest change in jaw movement
131 relating to particle breakdown and bolus formation. Gape cycles beyond cycle number 20 are

likely to be primarily for bolus formation and positioning before swallowing, and jaw movements are less likely to reflect differences in food material properties. Included gape cycles were also restricted to those starting and ending in the same position (maximum occlusion). The resulting data consisted of x, y, z coordinate data for each of the six landmarks for individual gape cycles throughout the chewing sequence.

Varying gape cycle durations resulted in differences in the number of equally temporally spaced frames in each cycle, and it was necessary to standardize the number of frames per cycle in order to make comparisons of homologous landmarks. The coordinates for each landmark were resampled and interpolated to obtain a total of 99 frames per cycle. This resulted in each gape cycle being represented as a motion path of 99 temporally evenly spaced three-dimensional marker coordinates for each of the six markers. To remove the effects of head movement during chewing, the 99 frame gape cycles were translated and rotated to three fixed facial landmarks averaged across all subjects (nasion, left and right condylion laterale). The first point of pogonion in each gape cycle was then translated to the coordinates 0, 0, 0. This registers the cycles among subjects such that pogonion with the mouth closed is coincident and the planes defined by the upper facial landmarks are parallel. This 'biomechanical space' registration preserves information about cycle size, shape, and orientation. We focused on movement of the pogonion point because it is furthest from the axis of rotation, although rigid-body motion of the mandible also resulted in associated movements at the right and left gonial landmarks. Landmarks were also extracted for each subject at the point of maximum occlusion (mouth closed). Three Euclidean distances and one angle were calculated from these landmarks: intergonial distance, pogonion to gonion, gonion to condylion laterale, and the gonial angle (Table 2).

155 *2.2 Application of geometric morphometrics to kinematics*

156 Previous multivariate approaches to kinematics have either been restricted to motions at a
157 joint (Park et al., 2005), or have utilized a Generalized Procrustes Analysis (GPA), thereby
158 removing biomechanically relevant differences in scale, position, and orientation (Slice 1999,
159 2002, 2003; Adams and Cerney, 2007; Pearson and Zumwalt, 2014). We adapt the geometric
160 morphometric toolkit to quantify and analyze whole motion paths (kinematics) in the Euclidean
161 space in which musculoskeletal mechanics operate, here called biomechanical space.
162 Biomechanical space is defined as the size and shape of a three-dimensional motion path for a
163 single point translated to a common fixed point (the point pogonion with jaws closed is taken as
164 the common start point for registration without scaling or rotation). Importantly, motion paths in
165 biomechanical space retain size, shape, and orientation and other biomechanically relevant
166 information such as velocity or posture.

167 *2.3 Within subject analyses (H1 and H2)*

168 In order to analyze how gape cycle size and shape varied across the chewing sequence
169 within each subject and food type, the coordinates of pogonion were averaged across the two
170 repeated chewing sequences for each cycle and food item (e.g., average of the two raw sweet
171 potato gape cycles for cycle number five). The resulting mean 1^{st} to 20^{th} gape cycles for raw
172 sweet potato and cooked sweet potato in each subject were used to test H1 and H2.

173 To test if gape cycles vary with cycle order across gapes 1-20 (H1), a multivariate
174 regression was used to regress averaged gape cycle coordinates on cycle number within each
175 subject. Significance of the regression was estimated using a permutation test (999
176 permutations). All multivariate regressions were carried out using the R package ‘geomorph’
177 (Adams and Otarola-Castillo, 2013). To test whether the relationship between gape cycles and

cycle number varies between food types within each subject, we calculated the angle between the regression vectors for each food type using a permutation test (999 permutations) in the R package 'morpho' (Schlager, 2017).

We assess the pattern of variation of gape cycles within the sample by carrying out a principal component analysis (PCA) (performed in "Geomorph," Adams and Otárola-Castillo, 2013). We visualize the variation in registered gape cycle coordinates between either extreme of the first principal component (PC1) and its relationship with cycle order. Importantly, the resulting principal components were only used as a visualization tool and not used to statistically compare cycle changes with order and food types. The eigenvalues, proportion of variance, and cumulative proportion of variance are listed in the Supplemental Online Material (SOM Table S1).

2.4 Among subject analyses (H3 and H4)

When registered to common points across individuals, gape cycle motion paths in biomechanical space also reflect differences in mid-facial form and gape cycle orientation. Although these differences were likely small within humans, we carried out a second set of analyses in Procrustes space to focus on differences in cycle size and shape alone. In order to transform the gape cycles from biomechanical space to Procrustes space we carried out a generalized Procrustes analysis (GPA) of gape cycle landmark coordinates and rescaled the resulting cycle shape coordinates by their centroid sizes. In the resulting Procrustes size and shape space, distances directly relate to relative landmark displacements between configurations. After pooling all individuals, gape cycle coordinates in biomechanical space and Procrustes size and shape space were separately averaged at each cycle number (1-20) for both raw and cooked sweet potato. This resulted in four datasets used to test H3 and H4: raw sweet potato in

biomechanical space, cooked sweet potato in biomechanical space, raw sweet potato in Procrustes space, and cooked sweet potato in Procrustes space.

Multivariate regressions and the angles between the food type regression vectors (described above) were used to assess the relationships between gape cycles and cycle number among individuals in biomechanical and Procrustes space (H3). Multivariate regressions with permutation tests (999 permutations, run in Geomorph) were used to test whether measures of mandibular morphology were correlated with gape cycle size and shape in biomechanical and Procrustes space. Gape cycle variation with cycle number and measures of mandibular morphology was visualized using a PCA (described above).

3. Results

3.1 Within subjects, gape cycles change across the chewing sequence (H1)

For both foods, gape cycles vary in form and orientation throughout the chewing sequence (Table 3). In six of the subjects, gape cycles for raw sweet potato covaried significantly with cycle number (Table 3). When chewing cooked sweet potatoes, gape cycles were significantly associated with cycle number in one of the subjects (Table 3).

3.2 Within subjects, cycles will vary with cycle number for raw and cooked sweet potato (H2)

Gape cycles, in biomechanical space, vary more for raw than cooked sweet potato across the chewing sequence. Half of the subjects had significantly different angles between the vectors of the regressions between cycle number and raw and cooked sweet potato gape cycles (Table 3). This indicates that gape cycles differ over time, between food types.

3.3 Among subjects, gape cycle variation with food type and cycle number is consistent (H3)

With all subjects combined, a multivariate regression of the average gape cycle sizes shapes and orientations (for cycle orders 1-20, in biomechanical space) on cycle number was

224 significant for cooked sweet potatoes ($p = 0.01$), but not raw sweet potatoes ($p = 0.55$). For
225 cooked sweet potato, gape cycles are larger at the beginning of the chewing sequence and
226 become narrower with increasing cycle number (Fig. 3A). The angle between the regression
227 vectors for each food type is significant ($p = 0.05$). A multivariate regression of the average
228 Procrustes aligned gape cycle sizes and shapes (1-20) on cycle number was significant for
229 cooked sweet potato ($p < 0.01$) but not for raw sweet potato ($p = 0.18$). Similar to biomechanical
230 space, cooked sweet potato gape cycles were wider at the beginning of the chewing sequence
231 (Fig. 3B). A permutation test on the angle between the regression vectors using the Procrustes
232 aligned coordinates was not significant ($p = 0.29$).

233 *3.4 Among subjects, gape cycles will covary with measures of mandibular size and shape (H4)*

234 Multivariate regressions with permutation tests of average raw and cooked sweet potato
235 gape cycles in biomechanical space on the distance between the right gonion to right condylion
236 laterale were not significant (Table 4). However, gape cycles significantly varied with intergonial
237 distance and the distance from pogonion to gonion for raw and cooked sweet potato (Fig. 4A-D).
238 Gape cycles also significantly varied with gonial angle for raw sweet potato (Fig. 4E). In all of
239 these relationships, narrower gape cycles were associated with larger pogonion to gonion and
240 intergonial distances when visualized along PC1. In multivariate regressions of Procrustes size
241 and shape variables with permutation tests on mandibular measurements, only the distance
242 between pogonion and gonion and intergonial distance achieved significance when chewing raw
243 sweet potato (Fig. 5A-B; Table 4). Longer pogonion to gonion and intergonial distances were
244 associated with narrower gape cycles (Fig. 5A-B).

245

246 **4. Discussion**

Studies relating variation in diet to mandibular morphology in primates have had varying success. Ross et al. (2012) propose that this is because diet influences mandibular morphology through other hierarchically-arranged variables such as ingestive behavior and jaw kinematics, along with their associated loading, stress, and strain regimes. Here we have addressed part of this relationship by examining how gape cycle variation differs between food types and across the gape cycle across and within individuals, and by evaluating the relationship between jaw kinematics and mandibular morphology. Our results reveal that mandibular morphology relates to differences in jaw movements, suggesting that investigations of diet and feeding behavior should consider possible impacts of mandibular morphology on behavioral variation. Future studies examining kinematic variation across individuals or taxa should also evaluate the influence of mandibular morphology on kinematic variation.

4.1 Within individuals, gape cycles vary with cycle number and food type (H1)

The results in Table 3 support the hypothesis that gape cycles vary across the chewing sequence in most subjects for raw sweet potato. This is consistent with previous studies suggesting that vertical displacement of the jaw and masticatory muscle activation decrease across a chewing sequence (Pruim et al., 1978; Manns et al., 1979; Hylander and Johnson, 1985; Spencer, 1998; Olmsted et al., 2005; Vinyard et al., 2008; Reed and Ross, 2010). Greater vertical jaw displacement at the beginning of the chewing sequence is thought to reflect the period of greatest food particle breakdown (Plesh et al., 1986; Foster et al., 2006; Woda et al., 2006; Vinyard et al., 2008; Reed and Ross, 2010; Laird et al., 2016). The lack of significant changes in gape cycle size and shape with cycle number in cooked sweet potato likely relates to the relatively soft food material properties of cooked sweet potato. Cooked sweet potato did not

require multiple chewing cycles in order to break the food into particles -- rather gape cycles were likely related to bolus formation.

4.2 Within individuals, gape cycle variation with cycle number differs for raw and cooked sweet potato (H2)

The regressions between cycle number and gape cycle size and shape differed between raw and cooked sweet potato in most individuals (H2, Table 3). Because the size and shape of the ingested food objects was uniform, gape cycle variation reflects differences in food material properties and bolus formation between raw and cooked sweet potato. Larger jaw vertical displacements have previously been associated with foods of higher toughness (Anderson et al., 2002; Foster et al., 2006; Wintergerst et al., 2008; but see Takada et al., 1994; Peyron et al., 1997). Additionally, the raw and cooked sweet potato regressions did not converge as cycle number progressed. This implies that preparation of a swallow-safe bolus from foods of different initial properties does not impose a common pattern of jaw kinematics after the initial food breakdown and bolus formation. It is possible that this result reflects our experimental setup as subjects generally swallowed the cooked sweet potato before the raw sweet potato. However, our results suggest that food material properties influence jaw movements and that these motions are incompletely described by vertical or lateral linear displacements (e.g., Reed and Ross, 2010; Laird, 2017). The consistency of covariation between gape cycles and food material properties requires further testing over a large range of food items.

4.2 Among individuals, gape cycle variation with cycle number and food type is consistent across subjects (H3)

We assessed the relationships between gape cycles and cycle number across all subjects. Gape cycles significantly varied with cycle number across subjects in cooked sweet potato and

292 there was a significant difference between the raw and cooked sweet potato vectors. This result
293 differs from the within subject analyses in that cooked sweet potato was only correlated with
294 cycle order in one subject (Table 3). This difference may reflect differences in bite conditions
295 across subjects that are beyond experimental control. For example, food positioning, food
296 fracture, and bite forces are unlikely to be consistent across subjects for a particular gape cycle
297 number. Regardless, the analyses both within and across subjects consistently showed diverging
298 regressions between raw and cooked sweet potatoes. Results from the Procrustes aligned
299 coordinates also significantly differed with chew number; however, the angle between the
300 vectors was not significantly different, suggesting that orientation and registration of cycles at
301 the pogonion with jaw closed account for the differences found in the among-subject between-
302 food cycles in biomechanical space.

303 *4.3 Among individuals, gape cycles covary with the size and shape of the face (H4)*

304 We explored covariation between mandibular size, shape, and orientation and gape cycles
305 using linear measures of mandibular morphology. We found that intergonial distance and the
306 distance from pogonion to gonion were related to gape cycle size and shape in both cooked and
307 raw sweet potatoes, and differences in the gonial angle were associated with gape cycle size and
308 shape in raw sweet potato. The gape cycles visualized on PC1 suggests subjects with longer
309 intergonial and pogonion to gonion distances and larger gonial angles have wider gape cycles.
310 Together, results from the biomechanical and Procrustes analyses suggest that gape cycle
311 variation with chewing sequence order and food material properties is mediated by differences in
312 the length and width of the mandible. When Procrustes size and shape variables were used to
313 describe motion cycles, a similar relationship was found for intergonial distance and the distance
314 from pogonion to gonion in raw sweet potatoes.

Our data suggest that gape cycle size and shape vary with size of the gonial angle, intergonial distance, and anteroposterior mandibular length (measured as pogonion to gonion), and covariation between gape cycles and mandibular morphology is consistent with previous proposals relating morphological variation to mechanical advantage. Subjects with acute gonial angles and broader mandibular breadth presumably have masseter and temporalis muscles that are positioned more anteriorly relative to the tooth row resulting in increased mechanical advantage and increased muscle activation (Herring and Herring, 1974; Throckmorton et al., 1980; Lindauer et al., 1993; Van Eijden and Turkawski, 2001; Hylander, 2013). We propose that smaller gape cycles were used in these subjects in order to maximize their mechanical advantage and minimize muscular stretch. Subjects with an obtuse gonial angle, smaller intergonial distance, and anteroposteriorly shorter mandibles may have had lower mechanical advantage, but they used larger gape cycles potentially allowing greater intraoral bolus manipulation. Further investigation of the morphological influences on jaw motions and bite force production is needed using taxa with varying mandibular morphology and data on individual variation in muscle mechanics (cf. Iriarte-Diaz et al., 2017).

Alternatively, changes in mechanical advantage may not be driving variation in jaw kinematics in modern humans. The magnitude of variation in jaw kinematics during normal chewing and mandibular morphology in modern humans may be small enough to not result in significant biomechanical differences in gape, muscle stretch, and mechanical advantage. This is consistent with suggestions that masticatory biomechanical constraints do not direct facial variation in *Homo sapiens* (Demes and Creel., 1988; O'Conner et al., 2005; Eng et al., 2013). Differences in gape cycle size and shape with mandibular morphology may instead reflect other factors such as relative differences in facial retraction, occlusal topography, or variation in

338 tongue manipulation of a food item. In order to assess whether mechanical advantage is an
339 important factor driving jaw kinematics, additional tests are needed using taxa with large
340 differences in facial prognathism and gape. Tests are also needed to examine the influence of
341 craniofacial morphology on aspects of feeding biomechanics outside of jaw kinematics, such as
342 chewing sequence duration, gape cycle length, or opening and closing length and velocity.
343 *4.4 Geometric morphometrics, kinematics, and application to fossil hominin form-function*
344 *relationships*
345 The development and application of geometric morphometric methods has transformed
346 quantitative approaches to comparative morphology. However, application of a geometric toolkit
347 to complex kinematic forms is less common and raises important questions regarding appropriate
348 methods. Here we present a novel application of geometric morphometric methods to the
349 quantification of kinematic variation. Our approach differs from previous methods in that the
350 orientations of the gape cycles are retained in biomechanical space, and the size and shape of the
351 whole gape cycle is treated as a single object, the motion cycle. This approach allows variation in
352 motion size and shape to be related to important variables in biomechanical space, including
353 muscular and bony morphology.
354 Previous studies on gape cycle kinematics have focused on maximum horizontal and
355 vertical displacement of the jaw (Reed and Ross, 2009; Iriarte-Diaz et al., 2010; Laird, 2017), but
356 our analyses suggest that the gape cycles undergo size and shape changes not captured by
357 maximum linear displacements. The position of maximum vertical and horizontal displacement
358 differed among subjects and across chew number. For example, maximum horizontal
359 displacement may occur closest to maximum gape in some subjects or closer to minimum gape
360 in others. This variation suggests maximum kinematic displacements may not be homologous

aspects of motion size and shape across individuals. Gape cycles also underwent size and shape changes outside of maximum displacement. Some gape cycles narrowed at maximum and minimum gape, whereas others maintained greater horizontal dimensions. This implies that displacements may not capture the subtleties of size and shape differences of three-dimensional kinematics. Our approach also compared among individual results in both biomechanical and Procrustes space. Overall, the results from biomechanical and Procrustes space were similar, but the angles between regression vectors of raw and cooked sweet potato gape cycle and chew number significantly differed in (H3), and fewer measures of mandibular morphology were significantly correlated with gape cycle size and shape in Procrustes space compared to biomechanical space (H4). This difference implies that gape cycle orientation influences some aspects of gape cycle variation.

This study demonstrates the utility and importance of employing a geometric morphometric toolkit to analyzing three-dimensional movements and its applicability to questions relevant to paleoanthropology. In particular, this approach allows a direct examination of covariation between movement and morphology that can be used to understand morphological and functional variation. For example, this approach can test how pelvic morphology covaries with locomotor gait in order to address the functional implications of pelvic variation in fossil hominins. This approach may potentially allow future studies to examine how complex movements relate to a range of variables including morphology, kinetics, and energetics.

381 **Figure Captions**

382 **Figure 1.** A sample chewing sequence with gapes 1-10 numbered. The x-axis is frames per
383 second (FPS). The y-axis is jaw displacement such that 0 is maximum jaw closure. A single gape
384 cycle, chew number 5, is demarcated by the gray area.

385

386 **Figure 2.** Six osteometric landmarks (A) and the location of the reflectors placed on the
387 overlying skin (B). Euclidean distances of mandibular morphology calculated from the marker
388 locations.

389

390 **Figure 3.** Visualization of the relationships between cooked sweet potatoes gape cycles in
391 biomechanical space (A) and Procrustes space (C and D) and chew number. Gape cycle size and
392 shape variation captured by the first principal component (PC1) are shown along the y-axes.

393

394 **Figure 4.** Visualization of correlations between gape cycles in biomechanical space and
395 measures of mandibular morphology. Gape cycle size and shape variation for raw sweet
396 potatoes (A, C, and E) or cooked sweet potatoes (B and D) are shown for the first principal
397 component (PC1) along the y-axes. Only significant relationships are shown.

398

399 **Figure 5.** Visualization of correlations between gape cycles in Procrustes space and measures of
400 mandibular morphology. Only significant relationships are shown. Gape cycle size and shape
401 variation for raw sweet potatoes are shown for the first principal component (PC1) on the y-axes.

402

403

404 **References**

405 Adams, D.C., Cerney, M.M., 2007. Quantifying biomechanical motion using Procrustes motion
406 analysis. Journal of Biomechanics 40, 437–444.
407 Adams, D.C., Otárola-Castillo, E., 2013. Geomorph: an R package for the collection and analysis
408 of geometric morphometric shape data. Methods in Ecology and Evolution 4, 393–399.
409 Ahlgren, J., 1966. Mechanism of mastication. Acta Odontologica Scandinavica 24, 1–109.
410 Anderson, K., Throckmorton, G.S., Buschang, P.H., Hayasaki, H., 2002. The effects of bolus
411 hardness on masticatory kinematics. Journal of Oral Rehabilitation 29, 689–696.
412 Bouvier, M., 1986a. A biomechanical analysis of mandibular scaling in Old World monkeys.
413 American Journal of Physical Anthropology 69, 473–482.
414 Bouvier, M., 1986b. Biomechanical scaling of mandibular dimensions in New World monkeys.
415 International Journal of Primatology 7, 551–567.
416 Bouvier, M., Hylander, W.L., 1981. Effect of bone strain on cortical bone structure in macaques
417 (*Macaca mulatta*). Journal of Morphology 167, 1–12.
418 Bramble, D.M., Wake, D.B., 1985. Feeding mechanisms of lower tetrapods. In: Hildebrand, M.,
419 Bramble, D.M., Liem, K.F., Wake, D.B. (Eds.), Functional Vertebrate Morphology.
420 Harvard University Press, Cambridge, pp. 230–261.
421 Cole, T.M., 1992. Postnatal heterochrony of the masticatory apparatus in *Cebus apella* and
422 *Cebus albifrons*. Journal of Human Evolution 23, 253–282.
423 Daegling, D.J., 1992. Mandibular morphology and diet in the genus *Cebus*. International Journal
424 of Primatology 13, 545–570.
425 Demes, B., Creel, N. 1988. Bite force, diet, and cranial morphology of fossil hominids. Journal
426 of Human Evolution 17, 657-670.

427 Foster, K.D., Woda, A., Peyron, M.A., 2006. Effect of texture of plastic and elastic model foods
428 on the parameters of mastication. Journal of Neurophysiology 95, 3469–3479.
429 Greaves, W.S., 1978. The jaw lever system in ungulates: a new model. Journal of Zoology 184,
430 271–285.
431 Herring, S.W., Herring, S.E., 1974. The superficial masseter and gape in mammals. The
432 American Naturalist 108, 561–576.
433 Hiiemae, K.M., 1978. Mammalian mastication: a review of the activity of the jaw muscles and
434 the movements they produce in chewing. In: Butler, P.M., Joysey, K.A. (Eds.),
435 Development, Function and Evolution of Teeth. Academic Press, London, pp. 359–398.
436 Hylander, W.L., 1979. The functional significance of primate mandibular form. Journal of
437 Morphology 160, 223–240
438 Hylander, W.L., 1985. Mandibular function and biomechanical stress and scaling. American
439 Zoologist, 25, 315–330.
440 Hylander, W.L., 1988. Implications of in vivo experiments for interpreting the functional
441 significance of “robust” australopithecine jaws. In: Grine, F.E. (Ed.), Evolutionary
442 history of the “Robust” Australopithecines. Aldine, Chicago, pp. 55–83.
443 Hylander, W. L., 2013. Functional links between canine height and jaw gape in catarrhines with
444 special reference to early hominins. American Journal of Physical Anthropology 150,
445 247–259.
446 Hylander, W.L., Johnson, K.R., 1985. Temporalis and masseter muscle function during incision
447 in macaques and humans. International Journal of Primatology 6, 289–322.
448 Ingervall, B., Helkimo, E.V.A., 1978. Masticatory muscle force and facial morphology in man.
449 Archives of Oral Biology 23, 203–206.

450 Ingervall, B., Thilander, B., 1974. Relation between facial morphology and activity of the
451 masticatory muscles. Journal of Oral Rehabilitation 1, 131–147.
452 Iriarte-Diaz, J., Reed, D.A., Ross, C.F., 2011. Sources of variance in temporal and spatial aspects
453 of jaw kinematics in two species of primates feeding on foods of different properties.
454 Integrative and Comparative Biology 51, 307–319.
455 Iriarte-Diaz, J., Terhune, C.E., Taylor, A.B., Ross, C.F., 2017. Functional correlates of the
456 position of the axis of rotation of the mandible during chewing in non-human primates.
457 Zoology 124, 106–118.
458 Katz, D.C., Grote, M.N., Weaver, T.D., 2017. Changes in human skull morphology across the
459 agricultural transition are consistent with softer diets in preindustrial farming groups.
460 Proceedings of the National Academy of Sciences 201702586, 1–6.
461 Kiliaridis, S., Engström, C., Thilander, B., 1985. The relationship between masticatory function
462 and craniofacial morphology: I. A cephalometric longitudinal analysis in the growing rat
463 fed a soft diet. The European Journal of Orthodontics 7, 273–283.
464 Kiliaridis, S., Kälebo, P. 1991. Masseter muscle thickness measured by ultrasonography and its
465 relation to facial morphology. Journal of Dental Research 70, 1262-1265.
466 Laird, M.F., 2017. Variation in human gape cycle kinematics and occlusal topography. American
467 Journal of Physical Anthropology 164, 574–585.
468 Laird, M.F., Vogel, E.R., Pontzer, H., 2016. Chewing efficiency and occlusal functional
469 morphology in modern humans. Journal of Human Evolution 93, 1–11.
470 Lindauer, S.J., Gay, T., Rendell, J., 1993. Effect of jaw opening on masticatory muscle EMG-
471 force characteristics. Journal of Dental Research 72, 51–55.

472 Lucas, P.W., 2004. Dental functional morphology: how teeth work. Cambridge University Press,
473 Cambridge.
474 Manns, A., Miralles, R., Palazzi, C., 1979. EMG, bite force, and elongation of the masseter
475 muscle under isometric voluntary contractions and variations of vertical dimension.
476 Journal of Prosthetic Dentistry 42, 674–682.
477 Møller, E., 1966. The chewing apparatus. An electromyographic study of the action of the
478 muscles of mastication and its correlation to facial morphology. Acta Physiologica
479 Scandinavica 280, 1–229.
480 Moss, M.L., Salentijn, L., 1969. The primary role of functional matrices in facial
481 growth. American Journal of Orthodontics 55, 566–577.
482 Nicholson, E., Harvati, K., 2006. Quantitative analysis of human mandibular shape using three-
483 dimensional geometric morphometrics. American Journal of Physical Anthropology 131,
484 368–383.
485 Olmsted, M.J., Wall, C.E., Vinyard, C.J., Hylander, W.L., 2005. Human bite force: the relation
486 between EMG activity and bite force at a standardized gape. American Journal of
487 Physical Anthropology 40, 160–161.
488 Park W., Martin B.J., Choe S., Chaffin D.B., Reed M.P., 2005. Representing and identifying
489 alternative movement techniques for goal-directed manual tasks. Journal of
490 Biomechanics 38, 519–527.
491 Pearson, O.M., Lieberman, D.E., 2004. The aging of Wolff's “law”: ontogeny and responses to
492 mechanical loading in cortical bone. American Journal of Physical Anthropology 125,
493 63–99.

494 Pearson Jr, W.G., Zumwalt, A.C., 2014. Visualising hyolaryngeal mechanics in swallowing
495 using dynamic MRI. Computer Methods in Biomechanics and Biomedical Engineering:
496 Imaging Visualization 2, 208–216.
497 Peyron, M.A., Maskawi, K., Woda, A., Tanguay, R., Lund, J.P., 1997. Effects of food texture
498 and sample thickness on mandibular movement and hardness assessment during biting in
499 man. Journal of Dental Research 76, 789–795.
500 Plesh, O., Bishop, W., McCall, W., 1986. Effect of gum hardness on chewing pattern.
501 Experimental Neurology 92, 502–512.
502 Pruim, G.J., Tenbosch, J.J., Dejongh, H.J., 1978. Jaw muscle EMG-activity and static loading of
503 mandible. Journal of Biomechanics 11, 389–395.
504 Ravosa, M.J., 1996. Jaw morphology and function in living and fossil Old World monkeys.
505 International Journal of Primatology 17, 909–932.
506 Ravosa, M.J., 2000. Size and scaling in the mandible of living and extinct apes. Folia
507 Primatologica 71, 305–322.
508 R Core Team, 2017. R: A language and environment for statistical computing. R Foundation for
509 Statistical Computing, Vienna.
510 Reed, D.A., Ross, C.F., 2010. The influence of food material properties on jaw kinematics in the
511 primate, *Cebus*. Archives of Oral Biology 55, 946–962.
512 Ross, C.F., Iriarte-Diaz, J., Nunn, C.L., 2012. Innovative approaches to the relationship between
513 diet and mandibular morphology in primates. International Journal of Primatology 33,
514 632–660.
515 Schlager, S., 2017. Morpho and Rvcg–Shape Analysis in R: R-Packages for geometric
516 morphometrics, shape analysis and surface manipulations. In: Zheng, G., Li, S., Székely,

517 G. (Eds.), Statistical Shape and Deformation Analysis: methods, implementation and
518 applications (pp. 217–256). Academic Press.
519 Smith, R.J., 1983. The mandibular corpus of female primates: taxonomic, dietary, and allometric
520 correlates of interspecific variations in size and shape. American Journal of Physical
521 Anthropology 61, 315–330.
522 Sockol, M.D., Raichlen, D.A., and Pontzer, H., 2007. Chimpanzee locomotor energetics and the
523 origin of human bipedalism. Proceedings of the National Academy of Sciences 104,
524 12265–12269.
525 Spencer, M.A., 1998. Force production in the primate masticatory system: electromyographic
526 tests of biomechanical hypotheses. Journal of Human Evolution 34, 25–54.
527 Spencer, M.A., Demes, B. 1993. Biomechanical analysis of masticatory system configuration in
528 Neandertals and Inuits. American Journal of Physical Anthropology 91, 1-20.
529 Takada, K., Miyawaki, S. Tatsuta, M., 1994. The effects of food consistency on jaw movement
530 and posterior temporalis and inferior orbicularis oris muscle activities during chewing in
531 children. Archives of Oral Biology 39, 793.
532 Taylor, A.B., 2002. Masticatory form and function in the African apes. American Journal of
533 Physical Anthropology 117, 133–156.
534 Taylor, A.B., 2006. Diet and mandibular morphology in African apes. International Journal of
535 Primatology 27, 181–201.
536 Throckmorton, G.S., Finn, R.A., Bell, W.H., 1980. Biomechanics of differences in lower facial
537 height. American Journal of Orthodontics 77, 410–420
538 Van Eijden, T.M.G.J., Turkawski, S.J.J., 2001. Morphology and physiology of masticatory
539 muscle motor units. Critical Reviews in Oral Biology Medicine 12, 76–91.

Vinyard, C.J., Wall, C.E., Williams, S.H., Hylander, W.L., 2003. Comparative functional analysis of skull morphology of tree-gouging primates. American Journal of Physical Anthropology 120, 153–170.

Vinyard, C.J., Wall, C.E., Williams, S.H., Hylander, W.L., 2008. Patterns of variation across primates in jaw-muscle electromyography during mastication. American Zoologist 48, 294–311.

White, T.D., Black, M.T., Folkens, P.A., 2011. Human Osteology. Academic press, Oxford.

Wintergerst, A.M., Throckmorton, G.S., Buschang, P.H., 2008. Effects of bolus size and hardness on within-subject variability of chewing cycle kinematics. Archives of Oral Biology 53, 369–375.

Woda, A., Mishellany, A., Peyron, M.A., 2006. The regulation of masticatory function and food bolus formation. Journal of Oral Rehabilitation 33, 840–849.

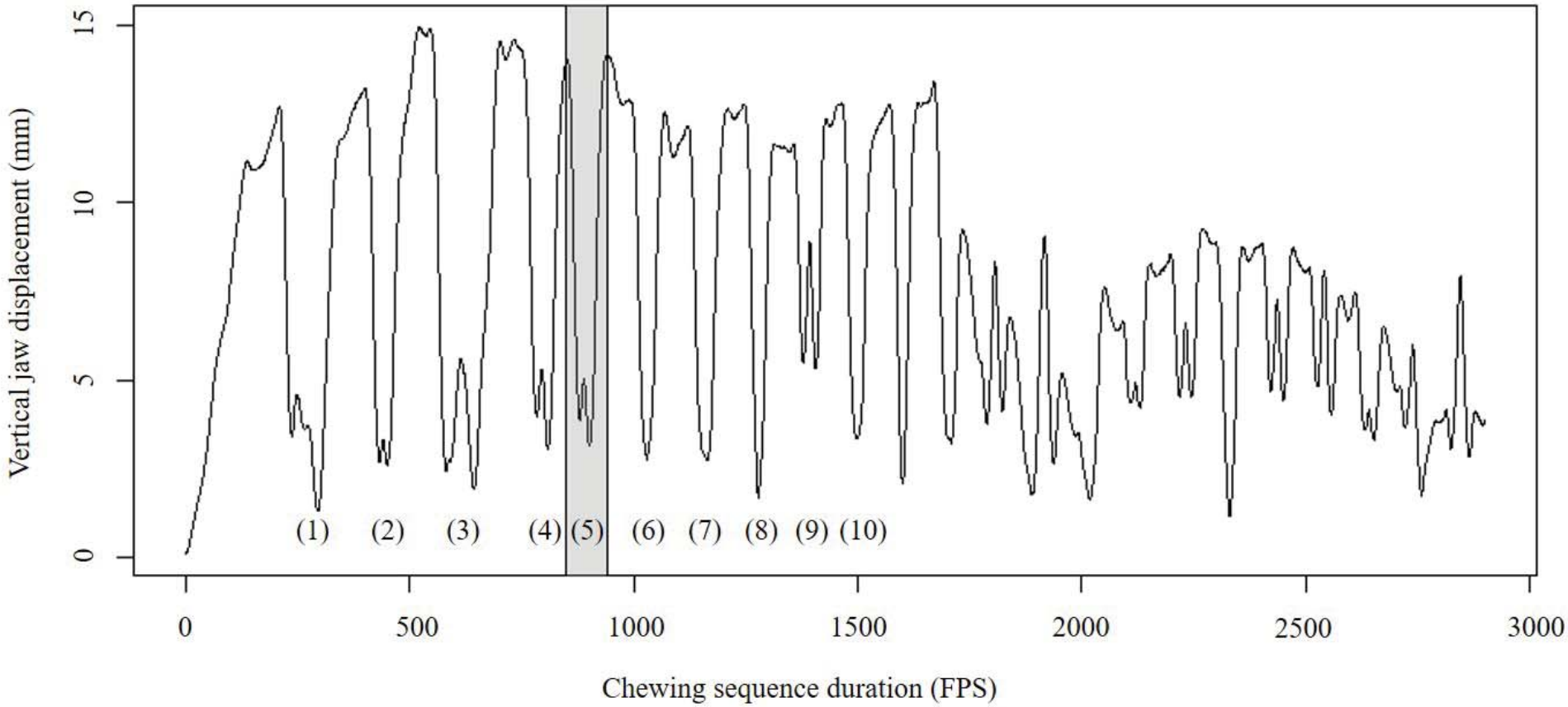
Vertical jaw displacement (mm)
0
5
10
15
(1)
(2)
(3)
(4)
(5)
(6)
(7)
(8)
(9)
(10)
0
500
1000
1500
2000
2500
3000
Chewing sequence duration (FPS)

A.

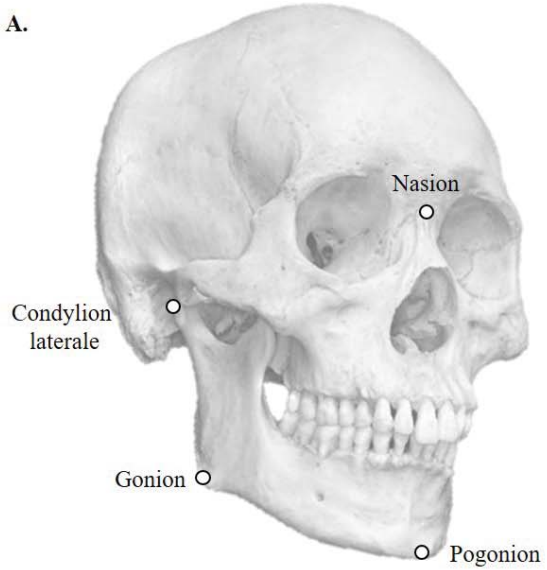
Nasion
Condylion laterale
Gonion
Pogonion

B.

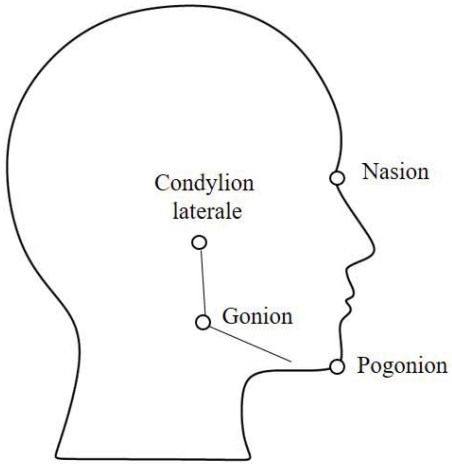
Condylion laterale
Nasion
Gonion
Pogonion

C.

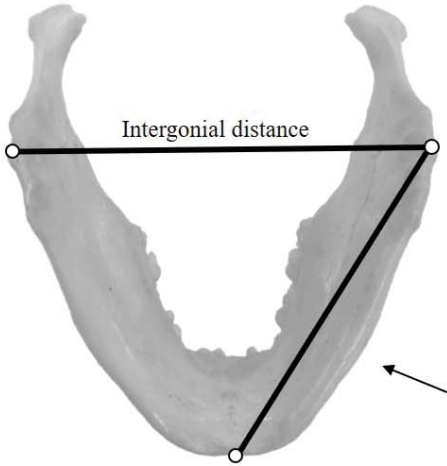
Intergonial distance

D.

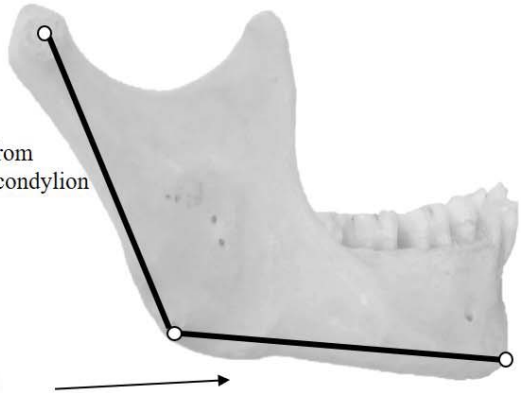
Distance from gonion to condylion laterale
Distance from pogonion to gonion

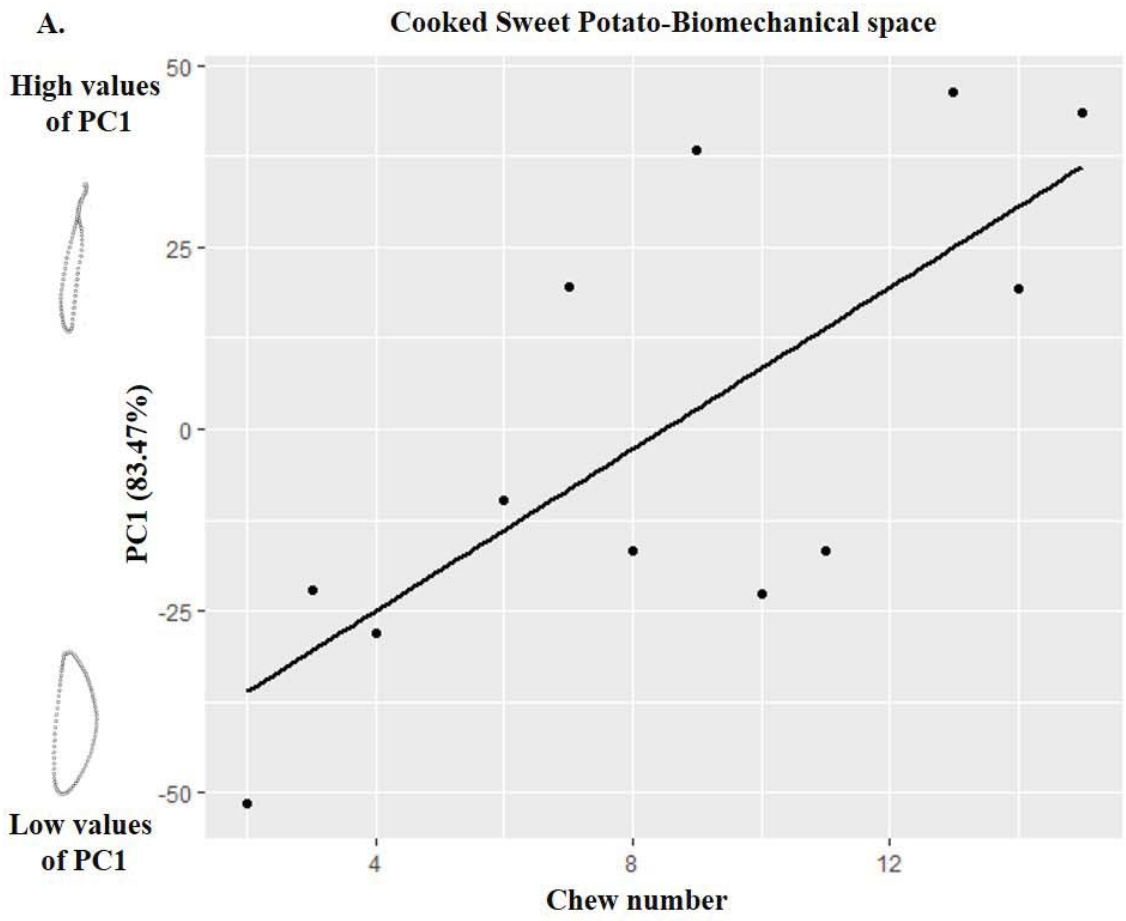
A.
Cooked Sweet Potato-Biomechanical space
High values of PC1
Low values of PC1
PC1 (83.47%)
50
25
0
-25
-50
4
8
12
Chew number

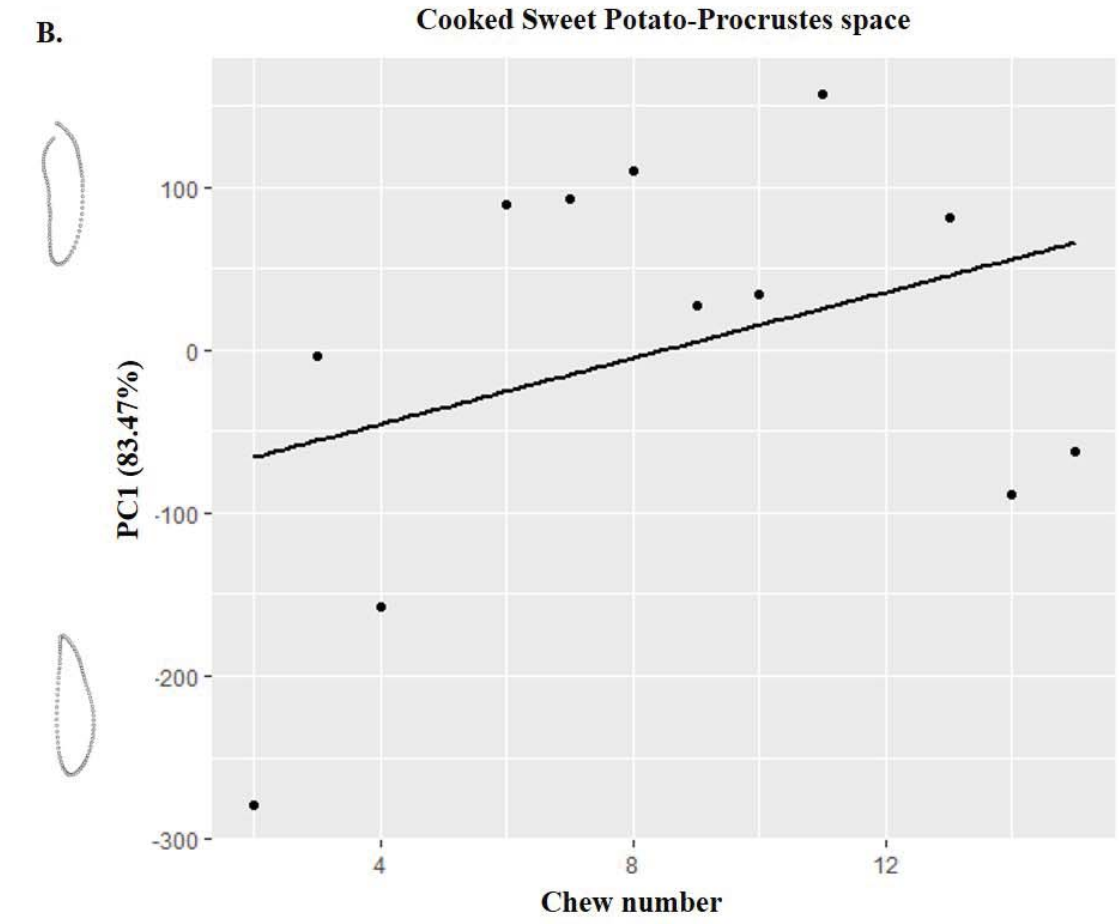
B.
Cooked Sweet Potato-Procrustes space
PC1 (83.47%)
100
0
-100
-200
-300
4
8
12
Chew number

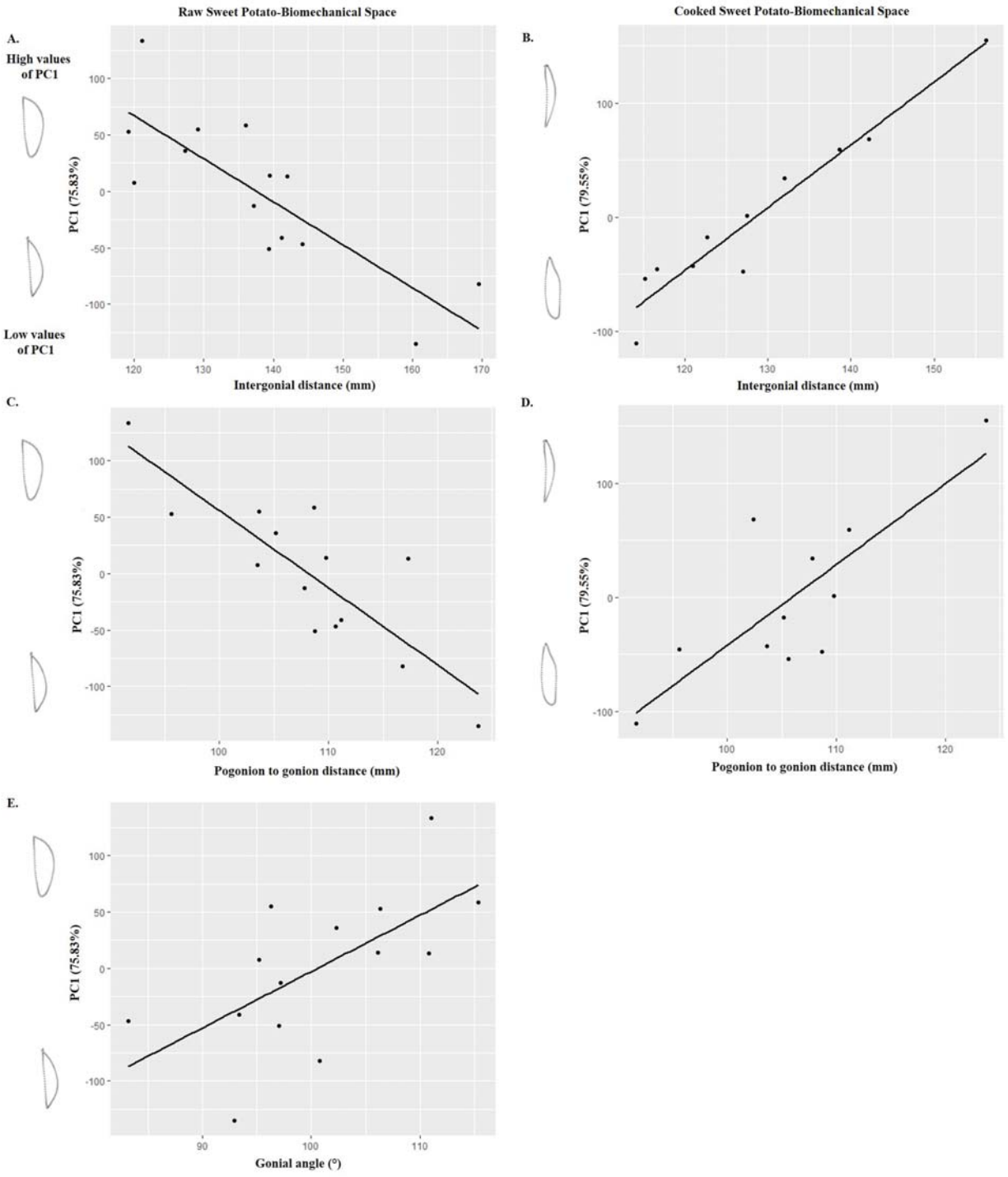
Raw Sweet Potato-Biomechanical Space
A.
High values of PC1
Low values of PC1
PC1 (75.83%)
Intergonial distance (mm)
Cooked Sweet Potato-Biomechanical Space
B.
PC1 (79.55%)
Intergonial distance (mm)
C.
PC1 (75.83%)
Pogonion to gonion distance (mm)
D.
PC1 (79.55%)
Pogonion to gonion distance (mm)
E.
PC1 (75.83%)
Gonial angle (°)

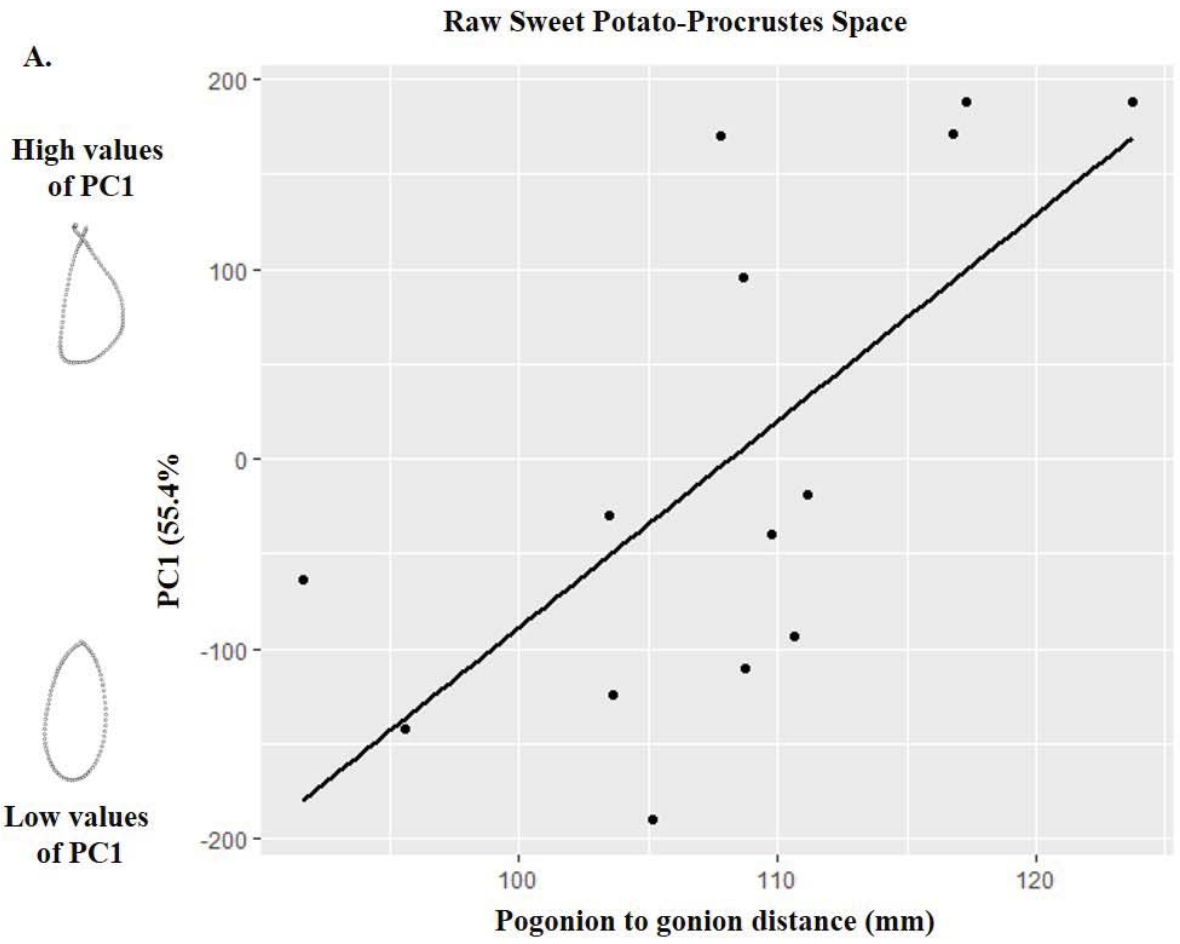
Raw Sweet Potato-Procrustes Space
A.
High values of PC1
Low values of PC1
PC1 (55.4%
200
100
0
-100
-200
100
110
120
Pogonion to gonion distance (mm)

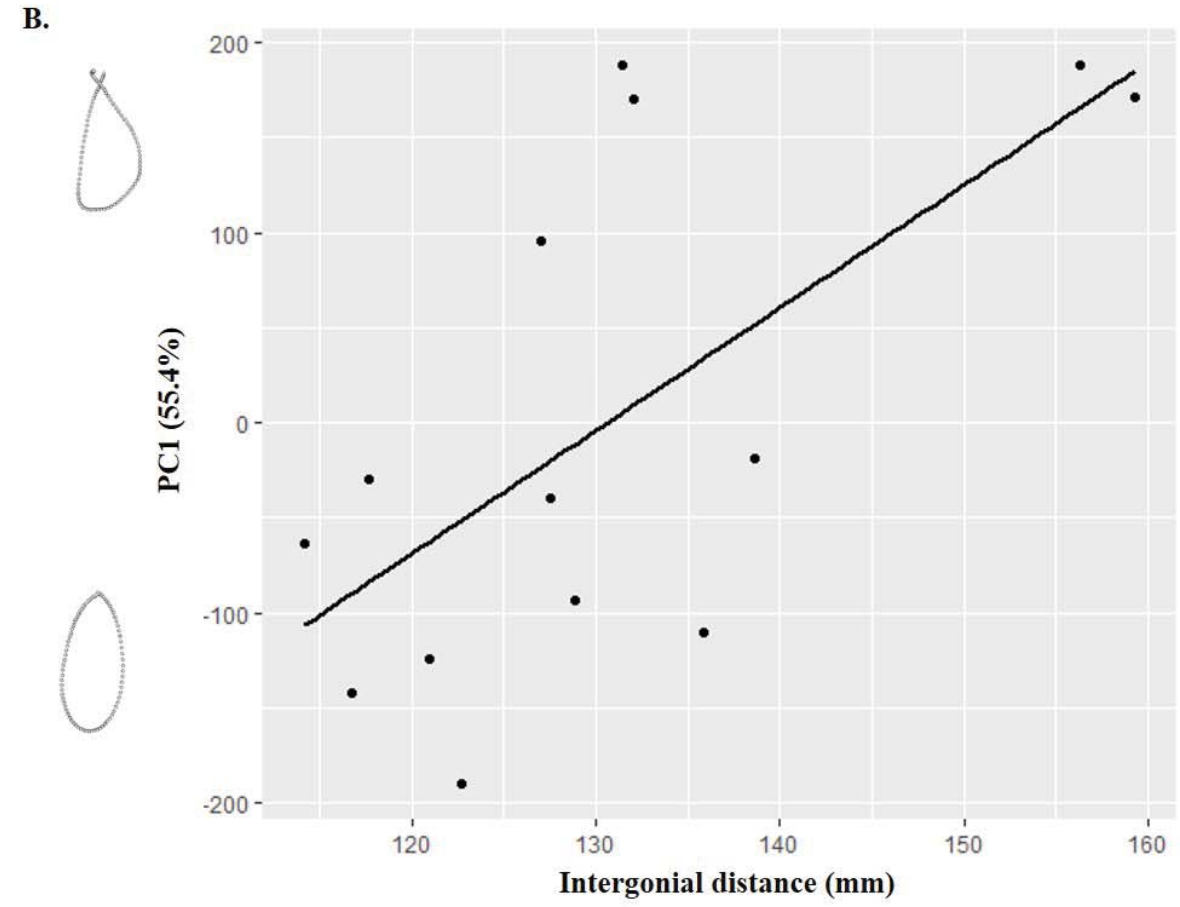
B.
PC1 (55.4%)
200
100
0
-100
-200
120
130
140
150
160
Intergonial distance (mm)

Supplementary Online Material (SOM):

Title page information (Removed for review).

SOM Table S1

Eigenvalues, Percentage of total variance explained, and cumulative variance from each of the principal component analyses used for visualization (Figure 3 and 4).

H3: RSP biomechanical space	Eigenvalue	Percentage of total variance explained	Cumulative variance explained
PC1	152.0388	0.7254	0.7254
PC2	41.94376	0.2001	0.9256
PC3	6.484204	0.03094	0.95651
PC4	3.636153	0.01735	0.97386
PC5	2.08895	0.00997	0.98383
PC6	0.916615	0.00437	0.9882
PC7	0.614844	0.00293	0.99114
PC8	0.56181	0.00268	0.99382
PC9	0.475245	0.00227	0.99609
PC10	0.2468	0.00118	0.99726
PC11	0.213435	0.00102	0.99828
PC12	0.196843	0.00094	0.99922
PC13	0.090222	0.00043	0.99965
PC14	0.039133	0.00019	0.99984
PC15	0.018692	0.00009	0.99993
PC16	0.010539	0.00005	0.99998
PC17	0.004772	0.00002	1

H3: CSP biomechanical space	Eigenvalue	Percentage of total variance explained	Cumulative variance explained
PC1	5518.93	0.7955	0.7955
PC2	1031.553	0.1487	0.9442
PC3	322.0342	0.04642	0.9906
PC4	40.66702	0.00586	0.99646
PC5	9.752504	0.00141	0.99787
PC6	8.529671	0.00123	0.9991
PC7	3.153998	0.00045	0.99955
PC8	1.883811	0.00027	0.99982
PC9	0.808057	0.00012	0.99994
PC10	0.406585	0.00006	1

H3: RSP Procrustes space	Eigenvalue	Percentage of total variance explained	Cumulative variance explained
PC1	2995.001	0.6937	0.6937

PC2	674.6383	0.1563	0.85
PC3	253.1268	0.05863	0.90864
PC4	161.4729	0.0374	0.946
PC5	79.17547	0.01834	0.96438
PC6	68.51403	0.01587	0.98025
PC7	29.17858	0.00676	0.98701
PC8	23.73346	0.0055	0.9925
PC9	9.28555	0.00215	0.99466
PC10	8.232768	0.00191	0.99657
PC11	4.418908	0.00102	0.99759
PC12	4.106581	0.00095	0.99854
PC13	2.742303	0.00064	0.99918
PC14	1.360676	0.00032	0.99949
PC15	1.060509	0.00025	0.99974
PC16	0.730615	0.00017	0.99991
PC17	0.405361	0.00009	1

H3: CSP Procrustes space	**Eigenvalue**	**Percentage of total variance explained**	**Cumulative variance explained**
PC1	16025.89	0.5853	0.5853
PC2	10116.44	0.3695	0.9548
PC3	630.2424	0.02302	0.97777
PC4	289.9633	0.01059	0.98836
PC5	170.8908	0.00624	0.99461
PC6	54.58978	0.00199	0.9966
PC7	44.27851	0.00162	0.99822
PC8	21.93986	0.0008	0.999
PC9	16.75298	0.00061	0.99963
PC10	6.56287	0.00024	0.99987
PC11	3.57331	0.00013	1

H4: RSP biomechanical space	**Eigenvalue**	**Percentage of total variance explained**	**Cumulative variance explained**
PC1	4643.1	0.7583	0.7583
PC2	1163.929	0.1901	0.9484
PC3	235.4313	0.03845	0.98688
PC4	35.46655	0.00579	0.99268
PC5	23.60162	0.00385	0.99653
PC6	8.572013	0.0014	0.9979
PC7	4.791984	0.00078	0.99871
PC8	3.113813	0.00051	0.99922

PC9	2.616242	0.00043	0.99965
PC10	1.086577	0.00018	0.99983
PC11	0.651766	0.00011	0.99993
PC12	0.274335	0.00004	0.99998
PC13	0.126323	0.00002	1

H4: CSP biomechanical space	**Eigenvalue**	**Percentage of total variance explained**	**Cumulative variance explained**
PC1	5518.93	0.7955	0.7955
PC2	1031.553	0.1487	0.9442
PC3	322.0342	0.04642	0.9906
PC4	40.66702	0.00586	0.99646
PC5	9.752504	0.00141	0.99787
PC6	8.529671	0.00123	0.9991
PC7	3.153998	0.00045	0.99955
PC8	1.883811	0.00027	0.99982
PC9	0.808057	0.00012	0.99994
PC10	0.406585	0.00006	1

Table 1. Reflective marker locations, landmark definitions (White and Folkens, 2000), and operational definitions applied here.

Marker location	Landmark Definition	Operational definition
Right and left condylion laterale	Most lateral point on the mandibular condyle at minimum gape	Subjects asked to repeatedly open and close their mouth; marker placed over condylion laterale at minimum gape.
Right and left gonion	Most posteroinferior point where the mandibular ramus meets the corpus	Marker placed over palpable gonion at minimum gape
Nasion	The intersection of the two nasal bones and frontal bone	Marker placed at the most posteroinferior midline point below glabella
Pogonion	The most anterior midline point on the chin	Marker placed over palpable pogonion point at minimum gape.

Table 2. Mandibular measurements from each subject taken when the jaw was in maximum occlusion.

	Pogonion to right gonion (mm)	Intergonial distance (mm)	Right gonion to right condylion laterale (mm)	Gonial angle (°)
Subject 1	103.48	117.68	71.80	95.16
Subject 2	108.70	126.98	73.27	115.40
Subject 3	116.82	159.30	72.81	100.75
Subject 4	91.62	114.17	55.48	111.08
Subject 5	111.15	138.64	56.50	93.33
Subject 6	123.76	156.28	58.39	92.93
Subject 7	103.62	120.95	61.66	96.32
Subject 8	109.77	127.53	62.87	106.12
Subject 9	95.61	116.71	61.12	106.36
Subject 10	110.65	128.89	73.06	83.15
Subject 11	102.41	142.18	69.55	111.65
Subject 12	107.78	132.02	67.52	97.19
Minimum	91.62	114.17	55.48	83.15
Maximum	123.76	159.30	73.27	115.40
Average	107.11	131.78	65.34	100.79
SD	8.69	14.82	6.77	9.49

Table 3. The results for H1 are *p*-values from permutation tests on the regression of gape cycles on gape cycle order and for raw sweet potato (RSP) and cooked sweet potato (CSP).

	Within-individuals: Gape cycle order~RSP (H1)	Within-individuals: Gape cycle order~CSP (H1)	Within-individuals: Angles between RSP and CSP regression (H2)[a]
Subject 1	0.81	-	-
Subject 2	**<0.01**[b]	**<0.01**	**0.04**
Subject 3	0.08	-	-
Subject 4	**<0.01**	0.08	**0.05**
Subject 5	**<0.01**	0.56	**0.03**
Subject 6	0.19	0.24	0.24
Subject 7	0.21	0.64	0.64
Subject 8	0.81	0.12	0.08
Subject 9	**<0.01**	0.50	0.06
Subject 10	0.22	-	-
Subject 11	**<0.01**	0.52	**-**
Subject 12	**0.02**	0.14	**0.03**

[a] The results for H2 are *p*-values from permutation tests on the angle between these regression vectors (CSP vs RSP).

[b]Significant results are shown in bold.

Table 4. Multivariate regressions *p*-values from permutation tests for gape cycles in biomechanical and Procrustes space and measures of mandibular morphology (H4).[a]

Biomechanical space	Raw sweet potato	Cooked sweet potato
Pogonion to right gonion	**<0.01**	**<0.01**
Intergonial distance	**<0.01**	**<0.01**
Right gonion to right condylion laterale	0.84	0.88
Gonial angle	**0.02**	0.21
Procrustes space	Raw sweet potato	Cooked sweet potato
Pogonion to right gonion	**0.01**	0.64
Intergonial distance	**0.02**	0.16
Right gonion to right condylion laterale	0.80	0.21
Gonial angle	0.85	0.73

[a]Significant values are shown in bold.